ISSN 1330–0008
CODEN FIZAE4

CHEMICAL AND SOLID STATE EFFECTS ON AUGER PROCESSES

LÁSZLÓ KÖVÉR

Institute of Nuclear Research of the Hungarian Academy of Sciences, P.O. Box 51, H-4001 Debrecen, Hungary

Received 7 April 1995

Revised manuscript received 24 May 1995

UDC 54.67, 54.68, 539.23

PACS 71.70.Ch, 82.80.Pv

Following a short review of the phenomena leading to changes in the Auger spectral distributions, it is demonstrated how Auger spectroscopy can be used for revealing the electronic structure local to the initial core hole and for obtaining information on hole–hole and electron–electron correlations. Using the Auger parameter concept, by the help of different Auger parameters, the initial and final state effects can be separated, the local screening and ligand polarizability can be characterized and the charge transfer can be determined. The advantages of the use of the X-ray excited Auger spectroscopy and cluster molecular orbital theoretical models in the studies of chemical and solid state effects on Auger processes are discussed. The power of these methods is illustrated by recent results obtained for metals, alloys and oxides, including materials of great practical importance.

1. Introduction

It is well known that Auger spectra of solids contain considerable information on chemical states and electronic structure of materials [1]. In recent years an increasing attention has been focused on extracting this information from the ex-

perimental data and a very significant progress has been made in understanding of the origin, magnitude and nature of the effects of chemical environment on Auger transition energies and probabilities, as reflected in recent reviews [2,3] and conference reports [4,5]. As a specific example for applications in important fields, the overview concerning the problem of the copper Auger data for high temperature superconductors [6] can be mentioned. Studying the effects of changes in the atomic surroundings of the core–ionized atom on the Auger spectra from molecules, clusters and solid surfaces is a wealthy source of information. These studies are leading to both providing a deeper insight into the Auger process itself in polyatomic systems and enhancing the possibilities of the chemical state analysis. In this report a summary of some recent results is presented in connection with the combined application of high resolution XPS and X–ray excited, high energy Auger spectroscopy of metals, alloys and insulators, using the cluster MO method in the interpretation of these data.

2. Effects of the atomic environment on Auger spectra excited from solids: basic physical phenomena

The transition energy E_{ijk} of the Auger process can be approximated by:

$$E_{ijk} = E_i - E_j - E_k - U_{jk}$$

where E_i and $E_{j,k}$ are the binding energies of the core level with the initial state hole and of the levels with the final state holes, respectively, while U_{jk} denotes the repulsion or correlation energy between the final state holes. In the case of Auger transitions involving core levels, it is generally a good assumption that the chemical shifts of the binding energies of these levels are similar, while in the case of core-valence transitions this assumption is usually not valid. Theoretical estimates of E_{ijk} can be obtained from the difference in total energies of the initial and final states determined by ab initio calculations. However, for polyatomic molecules or clusters this method is very time consuming and the convergence of the energy calculation is not always guaranteed [7]. The transition probability I_{ijk} of the ijk Auger process, using the simplest approach (independent particle frozen core approximation with the Wentzel Ansatz), can be expressed as [7]:

$$I_{ijk} = | < \Psi_f(i\epsilon)|e^2/r_{12}|\Psi_i(jk) > |^2$$

where ϵ is the energy of the ejected Auger electron, e^2/r_{12} is the Coulomb interaction between the two electrons participating in the transition and $\Psi_i(jk)$ and $\Psi_f(i\epsilon)$ are the wavefunctions of the initial and final states, respectively. From this simple picture, the highly local character of the Auger process is obvious. The probability of the Auger transitions involving levels of different neighbouring atoms is orders of magnitude smaller than the probability of the transitions taking place inside

the atom [7]. Therefore, strong effects of atomic environment on Auger transitions can be expected from the changes of the atomic initial and final states. Additional chemical dependence of Auger spectral distributions is coming from the appearance of the satellites due to the various initial and final state excitation processes accompanying the Auger process (initial state shake up/off, final state shake up/off) with spectator or participant electrons in the excited state [2,8]. A further process, which can influence strongly the relative Auger intensities, is the Coster Kronig transition involving a valence electron with varying localization, preceding the decay of the initial core hole [9]. Different hybridizations between the XPS core hole state and the Auger final state can also lead to satellite structures with relative intensities depending on the atomic environment [6]. Considerable line–broadening effects can appear as a consequence of the phonon generation due to core hole creation [10], while inelastic scattering (plasmon losses) processes in the solid can also result in changes of the lineshape. Auger chemical shifts, local electronic structure and correlation effects on core-valence Auger lineshapes will be discussed in detail below.

3. Wide energy range, X–ray excited Auger spectroscopy for studying chemical and solid state effects on Auger processes

Photon excitation has many advantages over electrons in producing Auger spectra in solids. Important for the detailed analysis of the Auger energies and lineshapes, the ionization cross section is high near threshold, the low background (compared to that in the case of the electron excited AES) and high peak to background ratio provide possibilities for achieving high energy resolution. X-ray induced Auger spectra suffer less from alterations in the chemical state of the surface components of the sample due to radiation effects, and smaller charging effect is expected, which makes possible the analysis of Auger spectra from insulators. A great benefit of the photon excitation is, however, the possibility of the use of continuum (bremsstrahlung, synchrotron) or wide energy band radiation which ensures efficient production of the Auger spectra in a very wide energy region [11]. From thin films deposited on low atomic number substrates good quality spectra (applicable for detailed analysis) can be obtained even at high (> 5 keV) transition energies [12]. The above advantages usually cannot be counterbalanced by the higher exciting flux and spatial resolution of the electron induced AES in this field.

4. Core Auger transitions: chemical shifts and Auger parameters

Core level chemical shifts are usually interpreted by means of the simplest electrostatic (point-charge potential) model describing the core level binding energy

as:

$$E_b(C) = E_b^0 + (V + kq),$$

where E_b^0 represents the contribution from the nucleus and the core electrons (the HF energy of the core electron C in the free atom), $V = \sum_j (q_j/R_j)$, the Madelung potential, q_j and R_j denote the charges on other atoms at distance R_j from the core ionized atom, k is the change in core potential resulting from the removal of a valence electron (charge transfer in the ground state) and q is the valence charge. Since in the above expression only initial state effects are considered [13], the binding energy can be written in a more complete form:

$$E_c(C) = E_b^0 + kq + V - R^{ea}$$

taking into account the polarization of the surrounding atoms upon the core hole creation, where R^{ea} represents the extra atomic relaxation (polarization or screening energy).

If the levels $C, C^{'}$ and $C^{''}$ are energy shifted nearly equally, changing the chemical environment of an atom, the change in the quantity defined as the Auger parameter [14]

$$\alpha^{'} = E_b(C) + E_k(CC^{'}C^{''})$$

will be given by:

$$\Delta\alpha^{'} \simeq 2\Delta R^{ea}(C^{'}) \simeq 2\Delta R^{ea}(C^{''}) \simeq -\Delta U(C^{'}C^{''}),$$

where ΔR^{ea} is the shift in the extra–atomic relaxation energy for an atom in two different chemical states. The chemical shifts in the XPS binding energies, Auger kinetic energies and Auger parameters can be conveniently presented in the form of chemical plots, greatly facilitating the identification of the different chemical species [14]. Initial state effects can be easily obtained from [13,15]:

$$E_k(CC^{'}C^{''}) = E_k^0 - 3E_b(C),$$

i.e. species with similar initial state effects (similar $(V + kq)$ values) are situated on the same $E_k = const - 3E_b$ line in the chemical plot. Figure 1. shows our results for Sn atoms in SnO and SnO_2 [15] where the initial state effects have been found to be similar.

G. Moretti [16] has developed a simple electrostatic model for characterizing the final state effects in the Auger process, assuming that the Auger parameter, and therefore R^{ea}, depend on different (local or non local) mechanisms of screening [17]. The local screening occurs when the screening ligand electron is transferred into a localized valence orbital of the core–ionized atom, and in this case the Auger

parameter is independent of the chemical state in the first approximation. However, in the case of non local screening, R^{ea} can be characterized by the electrostatic interaction between the core hole and nearest neighbour ligands [16]:

$$R^{ea} = (14.4/2)n\alpha/R^4[1 + D\alpha/R^3],$$

where α is the ligand electronic polarizability, R is the distance of the ligand from the core-ionized atom, D is a parameter [16] related to the local geometry and n is the number of the nearest–neighbour ligands.

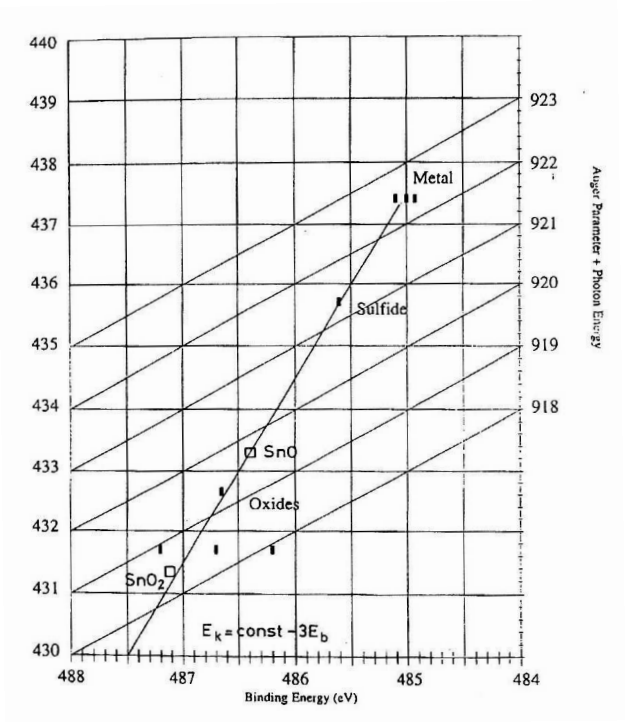

Fig. 1. Chemical state plot for Sn *compounds [15] (Handbook of X–Ray Photoelectron Spectroscopy, Perkin Elmer Co., Eden Prairie, U.S.A. 1992) with inclusion of the results of our measurements (open squares).*

Using the difference of the two Sn Auger parameters in SnO and SnO_2 from our experiment [15], the electronic polarizability of oxygen in SnO, as well as (by the help of the Clausius-Mossotti equation) the refractive index for SnO have been determined [15].

A more sophisticated analysis of $\Delta\alpha'$, in which k and q are assumed to depend linearly on the occupancy number N of the core orbitals, gives [3]:

$$\Delta\alpha' = \Delta\left[q\frac{\mathrm{d}k}{\mathrm{d}N} + \left(k - 2\frac{\mathrm{d}k}{\mathrm{d}N}\right)\frac{\mathrm{d}q}{\mathrm{d}N} + \frac{\mathrm{d}V}{\mathrm{d}N}\right]$$

where the first term originates from the relaxation due to the contraction of the occupied orbitals upon core ionization, the second describes the transfer of screening charge from the surroundings to the core–ionized atom, while the third term gives the polarization of the environment by the core hole.

The parameters k and $\mathrm{d}k/\mathrm{d}N$ can be determined by atomic structure calculations with correction for the compressed charge in solids [18]. In metals, the charge transfer Δq can be simply derived from [3]:

$$\Delta q = \frac{\Delta\alpha'}{(\mathrm{d}k/\mathrm{d}N)}.$$

It can be shown, assuming $k = k(q, N)$, that the initial and final state Auger parameters $\beta = E_k + 3E_b$ and $\alpha' = E_k + E_b$ can be separated and described by the help of potential parameters determined from atomic structure calculations [19].

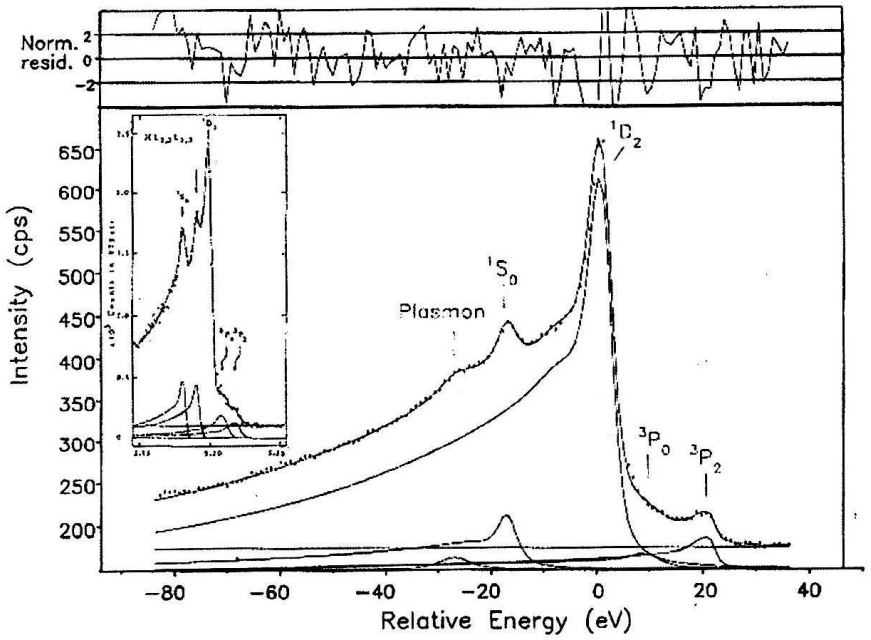

Fig. 2. Photoexcited Mn $KL_{2,3}$ $L_{2,3}$ *Auger spectrum compared with the spectrum obtained by Kovalik et al. (J. Electron Spectrosc. and Rel. Phenom. 50 (1989) 89) from Auger transitions following* ^{55}Fe *decay (inset) [12].*

As an example for the chemical information obtainable from deep core transition, the X-ray excited KLL Auger spectrum of manganese obtained from a thin film sample is shown in Fig. 2, in comparison with previous measurements [12]. These results helped the identification of a distinct chemical state (MnO) as a possible origin of the existence of an extra peak in the previous experiment [12].

5. *Core-valence Auger transitions: information on the local electronic structure and correlation effects*

Following the model of Ramaker [2], the core-valence Auger lineshapes can be determined on the basis of the *Final State Rule*: In the absence of significant configuration mixing (localization) and shake processes, the initial state determines separately the relative l or $l\,l^{'}$ (e.g. $l = s$ or p) Auger intensities; the shape of each contribution is determined by the final state DOS.

The experimental lineshapes $A(E)$ can be described as:

$$A_{ccv}(E) = C_s\rho_s^{'}(E) + C_p\rho_p^{'}(E)$$

and

$$A_{cvv}(E) = C_{ss}R_s^2\rho_s(E) \otimes \rho_s(E) + C_{sp}R_sR_p\rho_s(E) \otimes \rho_p(E) + C_{pp}R_p^2\rho_p(E) \otimes \rho_p(E),$$

where $\otimes$ denotes convolution integral, ρ_l ($\rho_l^{'}$) is the LDOS (screened DOS) of the final state without (with) core hole, C_i, C_{ij} denote atomic Auger intensities, normalized per filled shell, and the R_l factors provide the ratio of local charges in the screened initial state to that in the unscreened final state of the CVV process.

Correlation effects can be accounted for on the basis of the Cini–Sawatzky theory for final state hole–hole localization [20]:

$$A_{cvv}(E) \sim \frac{\rho \otimes \rho^{'}(E)}{[1 - \Delta U I(E)]^2 + [\Delta U \pi \rho \otimes \rho^{'}(E)]^2}$$

where $I(E) = \int(\rho \otimes \rho(E)/(E - \epsilon))\mathrm{d}\epsilon$ and ΔU is the effective hole–hole correlation parameter.

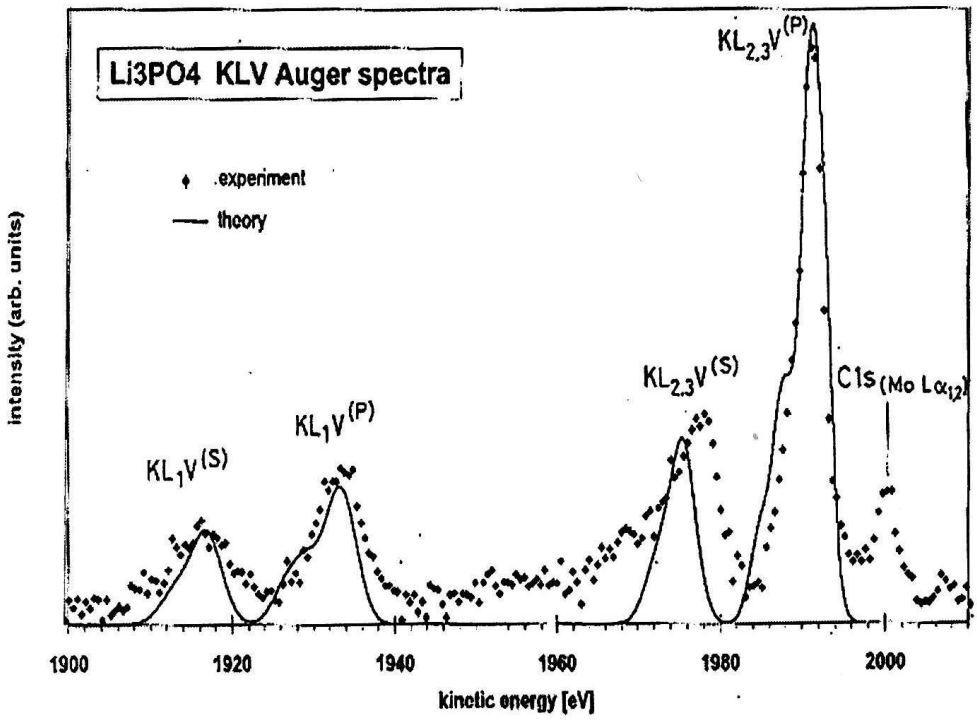

Fig. 3. Calculated P K*LV Auger spectra of* $Li_3rm\ PO_4$ *(solid line) in comparison with the respective experimental results (diamonds) [23].*

In the theoretical framework of our calculations of core–valence lineshapes, we applied the semiempirical approach above using the atomic Auger matrix elements. For calculating the LDOS distribution, the Discrete Variational Xα(DV–Xα) cluster molecular orbital method was applied [21] using a numerical basis set and the self–consistent charge scheme. For comparison with experimental high resolution XPS spectra, the local densities of states were obtained by replacing MO levels by energy distribution functions of Lorentzian shape of 2 eV widths. In the case of core–core–valence transitions, the core hole effects were accounted for by performing the cluster type calculations using a potential with a corresponding final state (L_1 or $L_{2,3}$) core hole, respectively.

Experimental Auger spectra were obtained by our home built high energy, high luminosity electron spectrometer [22], using Mo X-ray excitation.

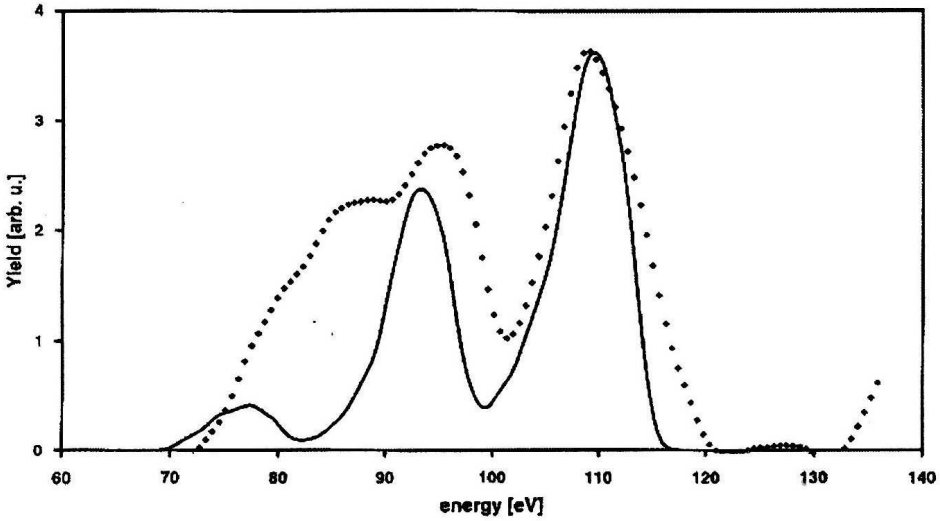

Fig. 4. Experimental P $L_{2,3}VV$ *spectrum of the* Na $(PO_3)_n$ *sample (diamonds), in comparison with the results of our cluster MO model calculations (solid line) [24].*

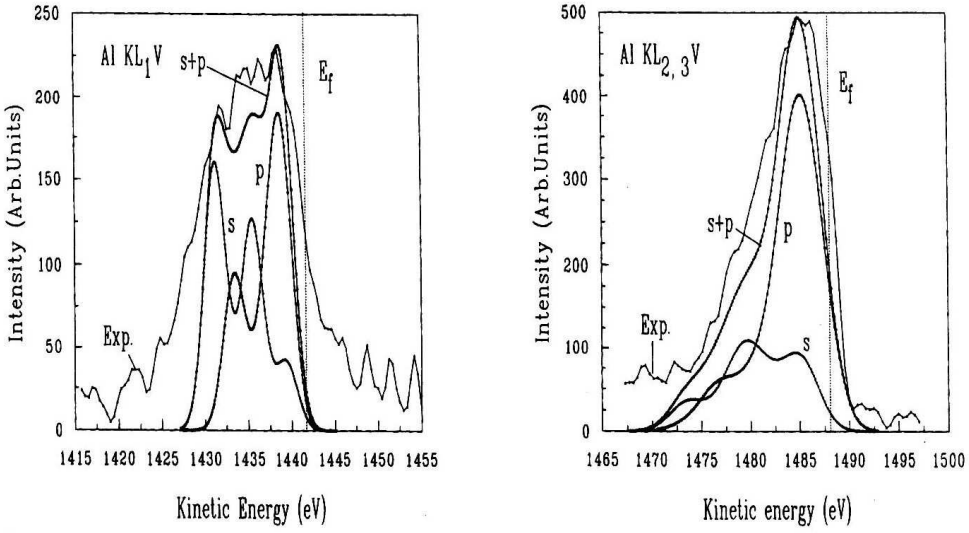

Fig. 5. Comparison of experimental and theoretical (cluster MO model) Al KLV *Auger spectra [25], a)* Al KL_1V *spectra, b)* Al $KL_2, 3V$ *spectra.*

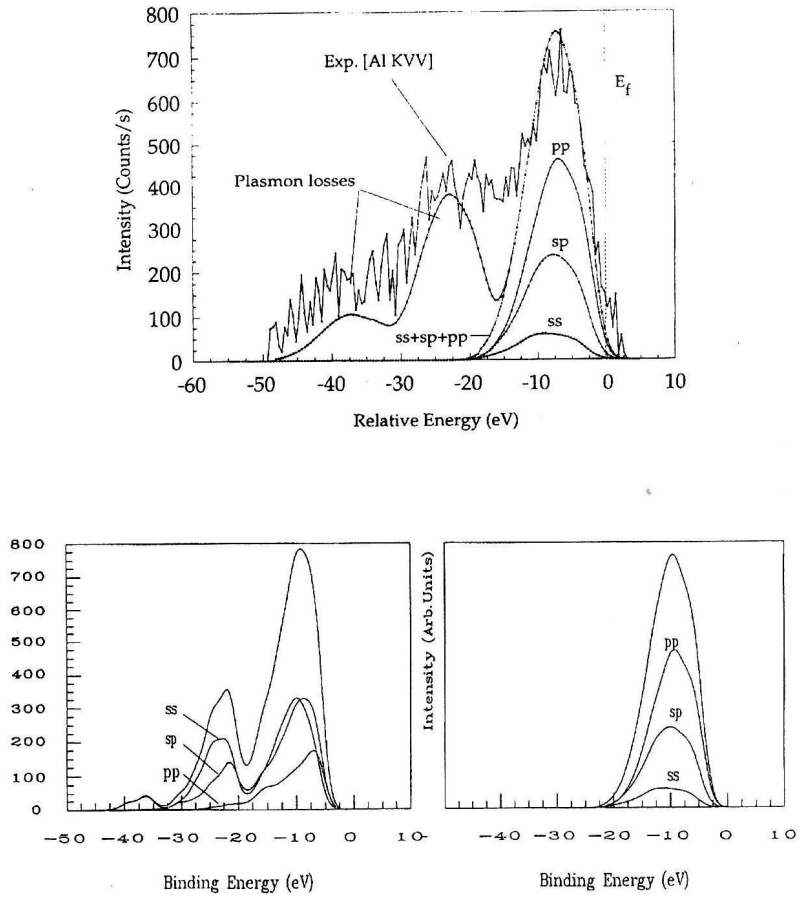

Fig. 6. Al *KVV spectra. a) Experimental* Al *KVV spectrum compared to the result from the cluster MO model [25], b) Calculated* Al K *VV spectrum of an* Al *surface with chemisorbed oxygen (top site) [26], c) Theoretical* Al K*VV spectrum from the cluster MO model [26].*

Our measured P KLV spectra [23] from various polycrystalline powder phosphorus oxyanion samples show the general features reflecting the dominance of the effect of the common Td symmetry. The P KLV spectrum of Li_3PO_4 is presented in Fig. 3 in comparison with the result of our calculation based on the semiempirical approximation described above. The relatively good agreement between the experimental and theoretical spectra demonstrates that, by using LDOS from MO cluster calculations and atomic Auger transition probabilities, the main structure of the KLV Auger spectra of phosphates can be explained. The same statement applies to the case of the P LVV spectra (Fig. 4) where both the energy separation between the two most intensive (ss and pp) peaks and the lineshape of the highest intensity line are well reproduced by our calculations [24].

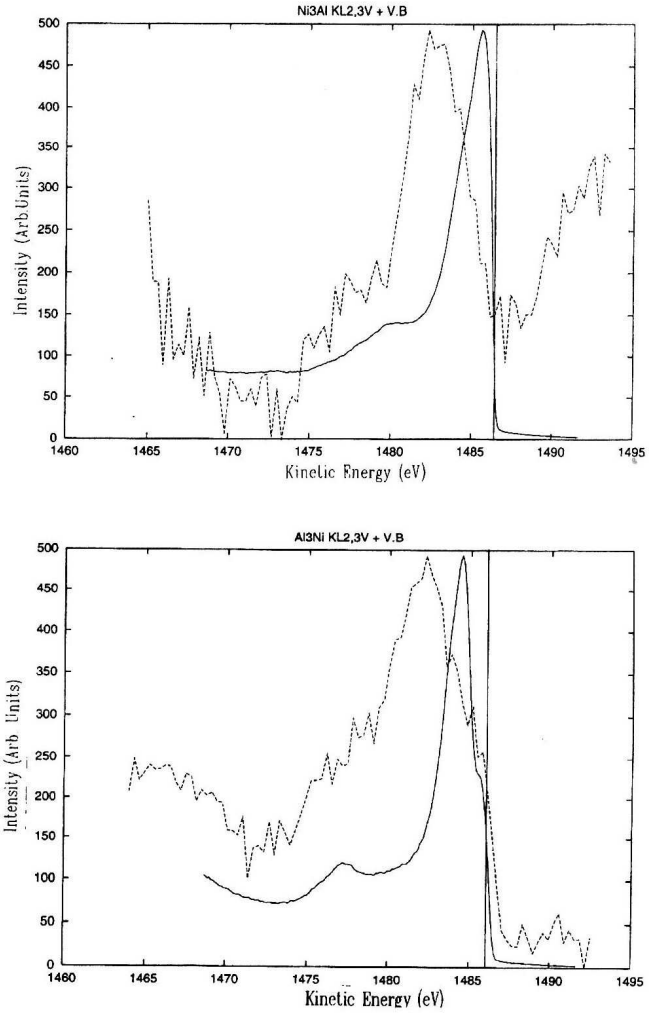

Fig. 7. Experimental Al $KL_{2,3}V$ *Auger spectra (dashed lines) of* AlNi *alloy samples, in comparison with the respective high resolution XPS valence band spectra (solid lines) [27]. The straight line marks the Fermi energy. a)* $AlNi_3$ *sample, b)* Al_3Ni *sample.*

While the Auger spectra of the phosphates show strong group localization, it is interesting to see the case of a simple metal with high conductivity. The comparison of the experimental and calculated KL_1V, $KL_{2,3}V$ and KVV spectra in Figs. 5 and 6a [25], demonstrates that our cluster MO model describes quite well both the KLV and KVV lineshapes in Al, predicting that the difference in the KL_1V and $KL_{2,3}V$ lineshapes is mainly due to the contribution from the s-type partial DOS, as well as the correct width of the KVV peak. Figures 6 b,c show the theoretical Al KVV

Auger spectra from the cluster MO model for Al surfaces with (Fig. 6b) and without (Fig. 6c) chemisorbed oxygen. The strong effect of the oxygen chemisorption (the effect of chemisorption is observable even at normal emission, as verified by the experimental shape) is due to the contribution from the O 2p level [26].

The theoretical LDOS functions are approximating well the Al KLV lineshapes in the strongly correlated Al_3Ni and $AlNi_3$ alloys. The experimental spectra from these samples, in comparison with our respective high resolution XPS valence band measurements, are shown in Figs. 7a,b [27].

In spite of involving valence electrons in the case of atomic-like transitions, as it has been demonstrated by Moretti [28] for oxygen containing compounds, the Auger parameter concept can be utilized for obtaining information on the polarizability of the chemical bond and on the oxygen final state hole-hole repulsion energies. Figure 8 shows a Moretti plot [28] with our experimental oxygen Auger parameter shifts for phosphates and tin oxides [23,15], demonstrating their low and high oxygen ion polarizabilities, respectively.

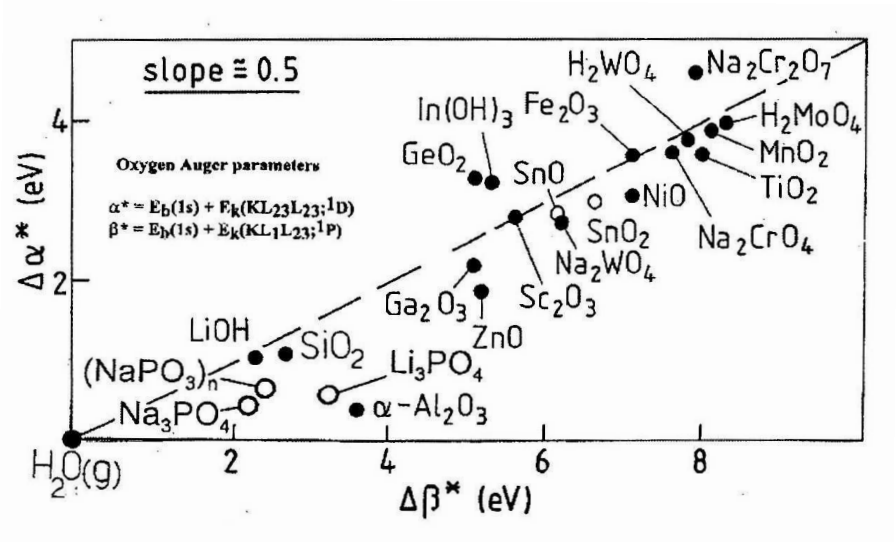

Fig. 8. Moretti plot for oxygen K-Auger parameters [28] including our experimental results obtained for phosphates and tin oxides [23,15].

Finally, as an example for influencing the core-valence relative Auger intensities by a preceding Coster-Kronig transition, the probability of which is strongly dependent on the localization of the valence electron involved, the case of the Tc can be mentioned, comparing the core $M_{4,5}$ spectra (obtained from internal conversion from ^{99m}Tc) of metallic Tc and NH_4TcO_4 samples [29].

The closing of the Tc M_4 M_5 $N_{4,5}$ CK channel in the case of the NH_4TcO_4 can be clearly observed from the disappearance of the CK broadening of the Tc M_4 line.

6. Summary

The methods of observation and interpretation of chemical and solid state effects on Auger transitions in solids were discussed and the use of the wide energy range X–ray excited Auger spectroscopy and the DV–Xα cluster model calculations for obtaining unique information on the local electronic structures in oxides, metals and alloys was demonstrated.

Acknowledgement

This work was partially supported by the following research projects: COST/D5-/12014 and OTKA/T00 7274/1993.

References

1) H. H. Madden, J. Vac. Sci. Technol. **18** (1981) 677;
2) D. E. Ramaker, Crit. Rev. in Solid State and Mater. Sci. **17** (1991) 211;
3) P. Weightman, J. Electron Spectrosc. and Rel. Phenom. **68** (1994) 127;
4) *Auger Spectroscopy and Electronic Structures*, G. Cubiotti, G. Mondio and K. Wandelt (eds.), Proc. of IWASES I (Springer Verlag, Berlin, 1989);
5) Proc. of IWASES II., K. Wandelt, C.O. Almbladh and R. Nyholm (Eds), Physica Scripta **T41** (1992);
6) D. E. Ramaker, J. Electron Spectrosc. and Rel. Phenom. **66** (1994) 269;
7) F. P. Larkins, ibid **51** (1990) 115;
8) U. Becker and R. Wehlitz, Physica Scripta **T41** (1992) 127;
9) N. Mårtensson and R. Nyholm, Phys. Rev. B **24** (1981) 7121;
10) J. A. D. Matthew, Phys. Rev. B **29** (1984) 3031;
11) L. Kövér, A. Némethy, I. Cserny and D. Varga, Surface and Interface Anal. **20** (1993) 659;
12) A. Némethy, L. Kövér, I. Cserny, D. Varga and P. B. Barna, J. Electron Spectrosc. and Rel. Phenom. **70** (1995) 183;
13) G. Moretti, in *Handbook of Heterogeneous Catalysis* (Eds.: G. Ertl, H. Knözinger ad J. Weitkamp) VCH Verlag, Weinheim, to be published;
14) C. D. Wagner, Discuss. Chem. Soc. **60** (1975) 291;
15) L. Kövér, G. Moretti, Zs. Kovács, R. Sanjinés, I. Cserny, G. Margaritondo, J. Pálinkás and H. Adachi, J. Vac. Sci. Technol A, in press;
16) G. Moretti, Surface and Interface Anal. **17** (1991) 352;
17) G. Moretti and P. Porta, ibid **15** (1990) 47;
18) T.D. Thomas and P. Weightman, Phys. Rev. B **33** (1986) 5406;
19) R.J. Cole, D.A.C. Gregory and P. Weightman, Phys. Rev. B**49** (1994) 7528;
20) M. Cini, Solid State Commun. **20** (1976) 655; G. A. Sawatzky, Phys. Rev. Lett. **39** (1977) 504;

21) H. Adachi, M. Tsukada and Satoko, J. Phys Soc Jpn. **42** (1978) 875;

22) L. Kövér, D. Varga, I. Cserny, J. Tóth and K. Tökési, Surface and Interface Analysis, **19** (1992) 9;

23) L. Kövér, A. Némethy, I. Cserny, A. Nisawa, Y. Ito and H. Adachi, ibid **22** (1994) 45;

24) L. Kövér, I. Cserny, A. Némethy and H. Adachi, ATOMKI Annual Report 1994, Institue of Nuclear Research of the Hungarian Academy of Sciences, Debrecen, in press;

25) Zs. Kovács, L. Kövér, D. Varga, P. Weightman, J. Pálinkás and H. Adachi, J. Electron Spectrosc. and Rel. Phenom. **72** (1995) 157;

26) Zs. Kovács, L. Kövér, D. Varga, P. Weightman, R. Sanjinés, G. Margaritondo, J. Pálinkás and H. Adachi, Proc. of the Third Internat. Workshop on Auger Spectroscopy and Electronic Structure, IWASES III, Univ. of Liverpool, 4-8 September 1994, p. 26;

27) Zs. Kovács, L. Kövér, P. Weightman, D. Varga, R. Sanjinés, G. Margaritondo, J. Pálinkás and H. Adachi, to be published;

28) G. Moretti, J. Electron Spectrosc. and Rel. Phenom. **58** (1992) 105;

29) L. Kövér, I. Cserny, V. Brabec, M. Fiser, O. Dragoun and J. Novák, Phys. Rev. B **42** (1990) 643.

KEMIJSKI EFEKTI I EFEKTI ČVRSTOG STANJA NA AUGEROVE PROCESE

Nakon uvoda o pojavama koje uzrokuju promjene Augerovih spektralnih raspodjela, opisuje se kako se Augerova spektroskopija može primijeniti za istraživanje lokalne elektronske raspodjele u odnosu na početnu šupljinu, kao i za podatke o korelacijama šupljina–šupljina i elektron–elektron. Primjenom Augerovog parametra mogu se razdvojiti učinci početnih i konačnih stanja, lokalno zasjenjenje i polarizivost liganada, te se može odrediti prijenos naboja. Moć tih metoda ilustrira se nedavnim rezultatima mjerenja za metale, legure i okside, uključivši neke materijale od velike praktične važnosti.